Flocking asbestos waste, an iron and magnesium source for Pseudomonas

Sébastien R. David, Sarah Fritsch, Anne Forster, Dris Ihiawakrim, Valérie Geoffroy

▶ **To cite this version:**

Sébastien R. David, Sarah Fritsch, Anne Forster, Dris Ihiawakrim, Valérie Geoffroy. Flocking asbestos waste, an iron and magnesium source for Pseudomonas. Science of the Total Environment, 2020, 709, pp.135936. ⟨10.1016/j.scitotenv.2019.135936⟩. ⟨hal-02981380⟩

HAL Id: hal-02981380

https://hal.science/hal-02981380v1

Submitted on 7 Mar 2022

HAL is a multi-disciplinary open access archive for the deposit and dissemination of scientific research documents, whether they are published or not. The documents may come from teaching and research institutions in France or abroad, or from public or private research centers.

L'archive ouverte pluridisciplinaire **HAL**, est destinée au dépôt et à la diffusion de documents scientifiques de niveau recherche, publiés ou non, émanant des établissements d'enseignement et de recherche français ou étrangers, des laboratoires publics ou privés.

Distributed under a Creative Commons CC BY-NC 4.0 - Attribution - Non-commercial use - International License

Version of Record: https://www.sciencedirect.com/science/article/pii/S0048969719359315
Manuscript_220f9e0fcc9dec6865878caa26b5f070

Flocking asbestos waste, an iron and magnesium source for Pseudomonas

Sébastien R. David[a,b], Sarah Fritsch[a], Anne Forster[a], Dris Ihiawakrim[c], and Valérie A. Geoffroy[a]*

a. Université de Strasbourg, CNRS-UMR7242, BSC, ESBS, 300 Blvd Sébastien Brant, 67413 Illkirch, Strasbourg, France

b. Agence de l'Environnement et de la Maîtrise de l'Energie, 20 avenue du Grésillé, BP 90406, 49004 Angers Cedex 01, France

c. Université de Strasbourg, CNRS-UMR7504, IPCM, 23 rue du Loess, BP 43, 67034 Strasbourg, France

* Corresponding author: V. A. Geoffroy, UMR 7242, Université de Strasbourg-CNRS, ESBS, Biotechnologie et Signalisation Cellulaire, Bd Brant, CS 10413, F-67412 Illkirch Cedex France.

Email: valerie.geoffroy@unistra.fr

Tel. (+33) 3 68 85 47 51

Fax (+33) 3 68 85 48 29

© 2019 published by Elsevier. This manuscript is made available under the CC BY NC user license
https://creativecommons.org/licenses/by-nc/4.0/

Abstract

Iron and magnesium are essential nutrients for most microorganisms. In the environment, the availability of iron is low relative to that of magnesium. Microorganisms have developed various iron acquisition systems, which have been well studied, whereas few studies have examined magnesium acquisition. The production of siderophores is one of the efficient strategies widely used to sustain iron nutritional requirements. Many studies have shown that minerals, such as clays, iron oxides, and silicates, can serve as nutrient sources for bacteria. Asbestos, a natural fibrous silicate present in soil contains iron and/or magnesium, depending on the species of asbestos. Our aim was to study the acquisition of iron and magnesium from flocking asbestos waste by *Pseudomonas aeruginosa* and the involvement of the siderophores, pyoverdine and pyochelin. Flocking asbestos waste promoted growth under iron- and magnesium-limited conditions, together with a decrease in pyoverdine production, correlating with the dissolution of iron from the waste. In long-term experiments, flocking asbestos waste provided these two essential elements for bacterial growth and resulted in a decrease of iron in asbestos fibers. Among the enzymes required for pyochelin and pyoverdine synthesis, PchA and PvdJ were tagged with the fluorescent protein mCherry to analyze the expression patterns of proteins involved in siderophore production. Both enzymes were produced in the presence of flocking asbestos waste, suggesting a role of the pyoverdine and pyochelin pathway in asbestos dissolution. We investigated the involvement of each siderophore in iron and magnesium removal using mutants in one or both siderophore pathways. We observed a significant increase in iron extraction in the presence of siderophores and the absence of one of the two siderophores could be compensated by the other. Flocking asbestos waste represents an iron and magnesium source for *P. aeruginosa*, with iron removal linked to a siderophore-driven mechanism.

Keywords

asbestos-*Pseudomonas*-siderophores-alteration-iron-magnesium

1. Introduction

Asbestos has been extensively used in many commercial products due to its unique properties. The two major waste products are cement asbestos waste and flocking asbestos waste (FAW) from insulation in buildings. Exposure to asbestos fibers can cause serious health problems, such as asbestosis and cancer, related to their physical and chemical factors. Asbestos toxicity correlates with the presence of iron as a catalyst of the Fenton reaction, leading to the generation of free radicals and reactive oxygen species (ROS) (Toyokuni, 2009). As a consequence of the associated health problems, asbestos was banned in many developed countries. However, following 30 years of intensive use, we are confronted with the generation of a vast amount of asbestos-containing waste. Today, most asbestos waste is typically disposed in controlled landfill sites, which does not remove the potential health risk of waste related to fiber inhalation. Asbestos consists of fibrous silicate minerals present in soil. There are two major families of asbestos i) serpentine, of which the only member is chrysotile, and ii) amphibole, among which the major members used industrially are crocidolite and amosite. The structure of chrysotile consists of a double layer comprised of a silicate sheet and brucite ($Mg(OH)_2$), in which the Si and Mg can be replaced by $Fe^{2+}$and Fe^{3+}, respectively (Virta, 2002). The surface of asbestos can also be contaminated by Fe, depending on where the asbestos was mined. Given the presence of Fe and Mg in the structure of asbestos, this mineral can be a nutrient source for microorganisms. Iron (Fe) and magnesium (Mg) are metals required for living organisms. They are present at different concentrations in the cell because of their specific physicochemical properties. Mg is found at high concentrations and is involved in basic cell metabolism, including the maintenance of macromolecules and bacterial walls and as cofactors for various enzymatic reactions (Groisman et al., 2013). Transition metals, such as manganese,

66 cobalt, nickel, copper, zinc, and iron, are present at lower concentrations in cells and have key
67 functions in many biological processes, such as energy production, oxido-reduction reactions,
68 and the stabilization of protein structures (Heldal et al., 1985). Iron, the fourth most abundant
69 metal in the Earth's crust, exists in two redox states, ferric (Fe^{3+}) and ferrous (Fe^{2+}), and is
70 involved in enzymatic processes, electron transfer, oxygen metabolism, and DNA and RNA
71 synthesis (Aguado-Santacruz et al., 2012; Andrews et al., 2003). Mg is more soluble than Fe
72 (Schvartz et al., 2005). Its solubility depends on the presence of oxygen and the pH (Cornell and
73 Schwertmann, 2003). Fe is poorly bioavailable in aerobic circumneutral environments and tends
74 to be limited by Fe(III)(hydr)oxide solubility. Microorganisms overcome the poor bioavailability
75 of iron by secreting low molecular-weight organic ligands, called siderophores, with a high
76 affinity for Fe^{3+} (Neilands, 1981). Siderophore production is well known among aerobic
77 microorganisms (Neilands, 1981), including fluorescent *Pseudomonas,* for which a wide variety
78 of siderophores has been described. More than 98% of fluorescent *Pseudomonas* isolated from
79 soil produce detectable siderophores under conditions of iron starvation (Cocozza and Ercolani,
80 1997). The range of siderophore concentrations found in soil is wide, from tens of micromoles to
81 a few millimoles per liter (Hersman et al., 1995). *Pseudomonas aeruginosa* is a ubiquitous
82 fluorescent *Pseudomonas* species found in diverse environments, such as water and the
83 rhizosphere (Goldberg, 2000), that adapts its iron-uptake strategy depending on the
84 environmental or infectious context (Cornelis and Dingemans, 2013). The iron uptake pathways
85 of this bacterium, known to be an opportunistic pathogen, are well characterized. *P. aeruginosa*
86 produces two siderophores, pyochelin (PCH), a low-affinity siderophore and a more energy-
87 demanding high-affinity molecule, pyoverdine (PVD) (Dumas et al., 2013). Pyoverdine consists
88 of three distinct structural entities i) a dihydroxy quinoline chromophore, which confers the color

89 and fluorescence of the molecule, ii) a peptide chain comprised of 6 to 12 amino acids bound to
90 its carboxyl group, and iii) a small dicarboxylic acid (or its monoamide) amidically connected to
91 the NH_2-group (Budzikiewicz, 2004, 1997; Budzikiewicz et al., 2007; Demange et al., 1990;
92 Fuchs and Budzikiewicz, 2001). Pyoverdine binds ferric iron with a high affinity (Ka = $10^{32}M^{-1}$)
93 in a 1:1 stoichiometric ratio via the catechol group of the chromophore and the two
94 hydroxyornithines of the peptide moiety (Albrecht-Gary et al., 1994). Pyochelin is a derivative of
95 salicylic acid, which chelates $Fe^{3+}$with an affinity of $10^{28.8}M^{-2}$ (Brandel et al., 2012) in a 2:1
96 (PCH:Fe^{3+}) stoichiometry. A tetra-dentate chelator is provided by one molecule of PCH and a bi-
97 dentate chelator by the second PCH to complete the hexacoordinate octahedral geometry
98 necessary for Fe^{3+}chelation (Tseng et al., 2006). Aside from iron, it has been shown that PVD
99 and PCH form stable complexes with other metal cations (Braud et al., 2009; Schalk et al.,
100 2011).

101 Microorganisms overcome the iron limitation in soil using siderophores to chelate iron
102 from Fe-bearing minerals. Indeed, siderophores play an important role in the formation of
103 soluble iron complexes for biological iron acquisition (Kraemer, 2004). Microbes then recover
104 ferric iron-siderophore complexes via cell-surface receptors. There is an abundant literature
105 concerning the weathering of minerals by biological processes. Deferoxamine-B, a bacterial
106 siderophore produced by *Streptomyces pilosus*, has been reported to enhance iron solubilization
107 of hornblende (Kalinowski et al., 2000) and kaolinite (Rosenberg and Maurice, 2003). Over the
108 last decades, mineral weathering of iron oxides, iron-rich aluminum silicates, and manganese
109 oxides by siderophore-producing bacteria has been well documented (Duckworth et al., 2009;
110 Maurice et al., 2009). *Pseudomonas* species have shown their ability to mobilize iron from iron
111 oxides, such as hematite or goethite by *Pseudomonas mendocina* (Hersman et al., 2001) or clay,

such as smectite by *Pseudomonas aeruginosa* (Ferret et al., 2014). Bacterial weathering of asbestos has also been recently reported. Several studies have investigated the biological alteration of raw asbestos or asbestos cement waste. Indeed, Bhattacharya et al. (2015) isolated well-adapted Gram-positive and Gram-negative bacteria from Indian asbestos mines that decrease the iron content of asbestos rocks, without identifying the species. Wang et al. (2011) and Wang and Cullimore (2010) showed that microorganism colonization induces porous structures in asbestos-cement pipes. Another Gram-positive bacteria, *Bacillus mucilaginosus*, promotes dissolution of serpentine powder by bacterial metabolites, most likely due to the production of organic acids and ligands, as suggested by Yao et al. (2013). Further studies on bacteria isolated from mines (Bhattacharya et al., 2015) showed the production of siderophores that may be involved in the weathering process, but with no characterization of their nature (Bhattacharya et al., 2016). Siderophore production has been shown in native asbestos, leading to iron dissolution from the fibers. Moreover, Rajkumar et al. (2009) described the plant growth-promoting mechanisms of rhizospheric bacteria in a serpentine soil, for which the secretion of siderophores is one of the various strategies used to release elements essential for plant growth. Direct evidence of iron removal by the siderophore deferoxamine from raw asbestos, chrysotile fibers (Mohanty et al., 2018), and amphibole fibers, such as crocidolite and amosite (Chao and Aust, 1994) has been shown. Importantly, the dissolution of iron by siderophores lowers the toxicity of the fibers of the three major commonly used species of asbestos, chrysotile (Poser et al., 2004), amosite (Gold J et al., 1997), and crocidolite (Gold J et al., 1997; Hardy and Aust, 1995; Poser et al., 2004).

To date, a few studies have focused on asbestos-cement waste, whereas none have focused on FAW. This anthropogenic material, used as insulation in buildings, is composed of

chrysotile fibers ($Mg_3Si_2O_5(OH)_4$, 5 to 90%) and gypsum ($CaSO_4$, $2H_2O$, 10 to 95%). The asbestos fibers present in FAW are only weakly bound in the gypsum, resulting in high emission of the fibers into the air. Here, we aimed to determine whether the aerobic *P. aeruginosa* can acquire Fe and Mg from FAW for growth and, at the same time, enhance FAW dissolution. We examined the role of pyoverdine and pyochelin in altering FAW. A better understanding of the bacterial alteration of asbestos waste may allow the development of an efficient bioremediation process, avoiding the continuing disposal of such waste in landfills.

2. Materials and Methods

2.1 Asbestos waste preparation

The flocking asbestos waste, chrysotile-gypsum, used in this work came from the asbestos removal site of Jussieu University of Paris and was kindly provided by the Mediterranean Company of Zeolites (SOMEZ). Asbestos samples (0.2 g) were sterilized by autoclaving (121°C for 20 min) and incubated at 70°C for 14 days before experiments for complete sterilization of the material. The heat removed all water, allowing precise weighing of the samples. Before each experiment, asbestos samples were washed with 20 mL sterile succinate or casamino acids (CAA) without magnesium to remove free Fe and Mg.

2.2 Bacterial strains, plasmids and growth conditions

The bacterial strains and plasmids used in this study are listed in Table 1. Stocks of bacterial strains were stored in LB-20% glycerol at -80°C. *Escherichia coli* was routinely grown in Luria Bertani medium (LB) at 37°C with shaking (220 rpm). *Pseudomonas* was routinely grown overnight at 30°C in Luria Bertani medium (LB) with shaking (220 rpm). Succinate (composition in $g.L^{-1}$: $K_2HPO_43H_2O$, 6.0; KH_2PO_4, 3.0; $(NH_4)_2SO_4$, 1.0; $MgSO_47H_2O$, 0.2;

158 sodium succinate, 4.0; pH adjusted to 7.0 by addition of NaOH) or CAA (composition in $g.L^{-1}$:
159 low-iron-casamino acids, 5.0; $K_2HPO_43H_2O$, 1.46; $MgSO_4.7H_2O$, 0.25) media were used as iron-
160 restricted media and sterilized using 0.2 µm polyethersulfone membrane filter units (Stericup
161 Merck). For iron and magnesium-depleted cultures, cells were harvested from a LB pre-culture
162 (24 h incubation), washed once with sterile succinate or CAA media not supplemented with
163 magnesium, and used to inoculate fresh succinate or CAA media without magnesium. The
164 cultures were incubated for 24 h at 25°C with shaking (200 rpm). For bacterial suspension, cells
165 were washed once with sterile iron- and magnesium-restricted medium and cell density adjusted
166 to an OD_{600} of 0.1, corresponding to $1\text{-}2.10^8$ $CFU.ml^{-1}$.

167 **2.3 Mutant construction**

168 All enzymes for DNA manipulation were purchased from Thermo Fisher Scientific and
169 used in accordance with the manufacturer's instructions. *E. coli* strain SM10 (Herrero et al.,
170 1990) was used as a host strain for the plasmid. DNA fragments from *P. aeruginosa* used for
171 cloning were amplified from the plasmid pLG45 *pvdJmcherry* using Phusion High-Fidelity DNA
172 polymerase (Thermo Fisher Scientific). The primers used are listed in Supplementary Table 1.
173 The procedure for the construction of the pLG45 *pvdJmcherry* plasmid involved amplification of
174 DNA fragments from *P. aeruginosa* and insertion of the *mcherry* gene flanked by upstream and
175 downstream regions of 700 bp, corresponding to the insertion site, into the pLG45 vector, as
176 previously described (Gasser et al., 2015).

177 The construction of the pEXG2 *pvdJmcherry* plasmid was obtained by amplification of
178 DNA fragments from pLG45 *pvdJmcherry* and their insertion into the pEXG2 vector (Rietsch et
179 al., 2005). Mutations in the chromosomal genome of *P. aeruginosa* were generated by

180 homologous recombination between the plasmid pEXG2 and the chromosome, with selection for
181 gentamicin resistance. Gene-replacement mutants were verified by PCR.

182 **2.4 Magnesium growth requirements for *Pseudomonas aeruginosa***

183 The *Pseudomonas aeruginosa* strain PAO1was cultured overnight at 30°C in LB medium
184 with shaking (220 rpm). The culture was centrifuged (10 min at 9,871 g) and washed twice with
185 succinate medium without magnesium. Bacterial cell density was adjusted to an OD_{600} of 0.01.
186 We dispensed 200 µl of the suspension into individual wells of a 96-well plate (Greiner, PS U-
187 bottomed microplate) with 0, 0.005, 0.05, 0.5, 1, 2, 5, and 20 $mg.L^{-1}$ $MgSO_47H_2O$,
188 corresponding to 0, 0.0005, 0.005, 0.05, 0.1, 0.2, 0.5, and 2 $mg.L^{-1}$ Mg. Plates were incubated at
189 30°C, with shaking, in a Tecan microplate reader (Infinite M200, Tecan) for measurements of
190 the OD_{600} at 30-min intervals, for 37.5 h. Assays were performed in triplicate.

191 **2.5 Expression of the pyoverdine and pyochelin pathway in the presence of FAW**

192 We analyzed the expression of the biosynthetic enzymes for siderophore production
193 using *Pseudomonas aeruginosa* PAO1 strains with the biosynthetic enzymes for pyochelin and
194 pyoverdine, PvdJ (this study) and PchA (Cunrath et al., 2015), tagged with the fluorescent
195 protein mCherry. Bacterial suspensions (20 mL) prepared in CAA medium without magnesium,
196 as described in paragraph 2.2, were incubated with chrysotile-gypsum samples. After 24 h of
197 incubation at 25°C with shaking (220 rpm), the number of bacteria was determined by serial
198 dilution, plating on LB-agar plates, and incubation at 30°C for 24 h. For the expression analysis,
199 the samples were centrifuged for 5 min at 67 g to separate the bacteria from the asbestos fibers.
200 Bacterial cells (100 µl) were dispensed into individual wells of a 96-well plate (Greiner, PS flat-
201 bottomed microplate). mCherry fluorescence (excitation/emission wavelengths: 570 nm/610 nm)

was measured in a Tecan microplate reader (Infinite M200, Tecan). Assays were performed using three to five replicates.

2.6 Asbestos dissolution by *Pseudomonas*

Microbial growth in the presence of flocking asbestos waste was assessed at 25°C with shaking (220 rpm) for 24 h. *Pseudomonas aeruginosa* PAO1 suspensions (20 mL), prepared in succinate medium without magnesium, as described in paragraph 2.2, were incubated with chrysotile-gypsum samples pre-treated by eight 24-h cycles with shaking (220 rpm) in succinate medium not supplemented with magnesium to remove free Fe and Mg. Controls without asbestos, supplemented or not with magnesium, were included. The number of bacteria was determined after 0, 4, 8, 12, and 24 h of incubation. Samples were serially diluted, plated on LB-agar plates, and incubated at 30°C for 24 h. The kinetics of iron and magnesium release from chrysotile-gypsum, with or without bacteria, were followed for 24 h by regular sampling at 0, 1, 2, 4, 6, 8, 12, and 24 h. Material was eliminated from supernatants by filtration (0.22 µm porosity). At the end of the experiment, cultures were gently centrifuged for 5 min at 67 g to separate the bacterial cells from asbestos fibers. Bacterial cells (10 mL) were centrifuged 10 min at 9,871 g, the pellets mineralized, and the supernatants filtered (0.22 µm porosity). The iron and magnesium content as well as the pH were measured and the amount of pyoverdine in solution in the supernatant estimated by monitoring the absorbance at 400 nm (Folschweiller et al., 2002). Assays were performed in three to five replicates.

Long-term alteration of chrysotile gypsum by *Pseudomonas aeruginosa* was performed by renewal cycles at 25°C with shaking (220 rpm). Controls without bacterial cells were included. Sixteen 8 h cycles were performed in the presence of 20 mL of bacterial cells prepared in succinate medium without magnesium, as described in paragraph 2.2, and reinoculated for

each renewal. For every cycle, bacterial enumeration was performed by serial dilution, plating on LB-agar plates, and incubation at 30°C for 24 h. Assays were performed in triplicate. Chrysotile fibers, with or without bacteria, were observed by transmission electron microscopy at the end of the experimental cycles.

The role of each siderophore in iron and magnesium dissolution from chrysotile-gypsum was evaluated using the wildtype *Pseudomonas aeruginosa* PAO1 strain (Stover et al., 2000) and three siderophore mutants: i) a pyoverdine-deficient strain (Δ*pvdF*) (Hoegy et al., 2009), ii) a pyochelin-deficient strain (Δ*pchA*) (Cunrath et al., 2015), and iii) a pyoverdine- and pyochelin-deficient strain (Δ*pvdF*Δ*pchA*) (Gasser et al., 2016). Bacterial suspensions (20 mL) prepared in CAA medium without magnesium, as described in paragraph 2.2, were added to chrysotile-gypsum samples. Controls without bacterial cells were included. After 18 h of incubation at 25°C with shaking (220 rpm), the number of bacteria was determined by serial dilution, plating on LB-agar plates, and incubating at 30°C for 24 h. The assays were gently centrifuged for 5 min at 67 g to separate the bacterial cells from asbestos fibers. Bacterial cells (10 mL) were centrifuged 10 min at 9,871 g, the pellets mineralized, and the supernatants filtered (0.22 µm porosity). The iron and magnesium content as well as the pH were measured. Assays were performed in triplicate.

Bacterial pellets were mineralized by washing them once with ultra-pure water and drying at 50°C for 48 h. Cells were mineralized by incubation in 77 µL 65% (v/v) HNO_3 for 48 h at room temperature. The volume was brought up to 5 ml with ultra-pure water to obtain 1% HNO_3 and the samples filtered through a membrane with a 0.22 µm filter unit.

2.7 Determination of Fe and Mg content

The iron content was determined using the bathophenanthroline method, which is a sensitive colorimetric method for determining ferrous iron content. Total iron was determined by converting ferric iron to ferrous iron using thioglycolic acid. Each sample was analyzed in triplicate. Samples (20 µL) were dispensed into each well of a 96-well plate (Greiner, PS flat-bottomed microplate) and 40 µL saturated sodium acetate (5.5 M) (Sigma-Aldrich), 80 µL cold distilled water, 10 µL thioglycolic acid solution diluted 10 times in water (Sigma-Aldrich), and 10 µL bathophenanthroline (5 $mg.mL^{-1}$) (Sigma-Aldrich) added per well. After shaking, microplates were stored overnight at 4°C. Absorbance was measured at 535 nm in a Tecan microplate reader (Infinite M200, Tecan) and iron concentration ($mg.L^{-1}$) determined by comparing the values to those of a standard reference curve.

For magnesium content, the calmagite method was used. Magnesium forms a colored complex with calmagite. Ethylene glycol tetra acetic acid (EGTA) was used to eliminate any calcium interference. Each sample was analyzed in triplicate. The reactive solution was prepared by mixing one volume of reagent 1 (1 $mol.L^{-1}$ 2-Methyl-2-Amino-1-Propanol and 215 $\mu mol.L^{-1}$ EGTA) with one volume of reagent 2 (300 $\mu mol.L^{-1}$ calmagite). Samples (3 µL) were dispensed into each well of a 96-well plate (Greiner, PS flat-bottomed microplate) and 300 µL reactive solution mix added. After shaking and 30 s of incubation, absorbance was measured at 500 nm in a Tecan microplate reader (Infinite M200, Tecan) and the magnesium concentration ($mg.L^{-1}$) determined by comparing the values to those of a standard reference curve.

2.8 STEM-EDX of asbestos fibers

Transmission electron microscopy (TEM) images were recorded with a JEOL 2100 microscope using a 200-kV potential applied to a LaB6 filament as an electron source. Resolution of the TEM was 0.21 nm. TEM mapping was performed in scanning transmission

electron microscopy (STEM) mode (resolution 2 nm) using a silicon drift detector-energy dispersive X-ray (SSD-EDX) spectrometer to determine the chemical composition.

2.9 Statistical analysis

Results presented in all figures correspond to the mean values of three to five replicates. The Kruskal-Wallis test (R version 1.0.153) followed by a Conover post-hoc analysis was used to determine differences among values of pyoverdine production after bacterial growth, with or without asbestos fibers, and magnesium extraction from chrysotile-gypsum after incubation in the presence of WT or mutant *P. aeruginosa* PAO1. Differences in the iron dissolution from chrysotile-gypsum after 24 h of bacterial growth were determined using the Wilcoxon signed rank test (R version 1.0.153). One-way ANOVA (R version 1.0.153), followed by Tukey's post-hoc analysis was used to determine differences in mCherry fluorescence levels after bacterial growth in the presence of asbestos and differences in iron extraction from chrysotile-gypsum after incubation in the presence of WT or mutant *P. aeruginosa* PAO1. Values with the same letter are not significantly different ($p > 0.05$).

3. Results and Discussion

3.1 Microbial growth in the presence of FAW

Wildtype cultures of *Pseudomonas aeruginosa* were grown in medium depleted of magnesium and iron, with or without FAW. This waste contains asbestos fibers of chrysotile and gypsum, potentially containing iron and magnesium that could be used as nutrient sources by *P. aeruginosa*. We observed no growth after 24 h of incubation in minimal succinate medium depleted of magnesium and iron (Succ-Mg) (**Figure 1A**). Growth was restored after 8 h of

292 incubation in the positive control in succinate medium (Succ). Thus, magnesium is essential for
293 optimal bacterial growth. The number of bacteria decreased in the first hours of culture in the
294 Succ-Mg medium supplemented with FAW, probably due to the adsorption of bacterial cells to
295 the waste. Microbial attachment to mineral surfaces leads to the formation of a
296 microenvironment that confers protection to microorganisms against environment stress
297 (Beveridge et al., 1997; Liermann et al., 2000; Ojeda et al., 2006). As a consequence, mineral
298 nutrients can be extracted directly by some microorganisms. *Pseudomonas* shares the same
299 mechanism as many soil bacteria that promote mineral weathering by the production of
300 siderophores to overcome iron limitation. After 12 h, the number of planktonic cells reached the
301 same level as that of the initial inoculum and showed growth similar to the positive control at 24
302 h. This shows the ability of *P. aeruginosa* to use magnesium present in the FAW as a nutrient
303 source. Thus, bacteria can alter asbestos waste, showing the feasibility of the biological treatment
304 of asbestos.

305 We determined the amount of the exogenous siderophores pyoverdine and pyochelin for
306 all conditions. Similar amounts of pyochelin were observed in Succ-Mg medium, with or without
307 FAW, after 24 h (110-130 µM) (data not shown), whereas the levels of pyoverdine varied widely
308 between conditions (**Figure 1B**). *P. aeruginosa* cultures grown in Succ medium produced a
309 cumulative pyoverdine concentration of 183 µM as a consequence of iron depletion of the
310 medium. In contrast, only 2 µM of pyoverdine was produced in Succ-Mg medium related to the
311 absence of bacterial growth. Supplementation with FAW resulted in a lower pyoverdine
312 concentration (27 µM) than that of the positive control, whereas growth was similar. The
313 pyoverdine pathway is well known to be repressed by the presence of iron. Our results show a
314 decrease of pyoverdine production, suggesting that dissolved iron was released from the FAW,

315 repressing the pyoverdine system. Indeed, *P. aeruginosa* has already been reported to use iron
316 from smectite, a type of clay, by the siderophore acquisition system (Ferret et al., 2014), similar
317 to the repression of the pyoverdine pathway and stimulation of growth that we observed.
318 We measured the amount of iron and magnesium in the bacterial cells and supernatant
319 (**Figure 1C**). The concentration of total iron was significantly higher in the presence of bacteria
320 (0.27 mg/L) than the control (0.06 mg/L), FAW incubated in sterile medium. The supernatant
321 contained 0.09 mg/L iron, whereas more iron accumulated in the bacterial cells (0.18 mg/L). As
322 iron is an essential element required for bacterial metabolism, bacteria regulate the intracellular
323 iron concentration and can store it, as well several other elements. Cunrath et al. (2016) focused
324 on the metallome of *P. aeruginosa* and showed that the ratio between the metal concentration in
325 bacteria and that in growth medium are not equivalent. They showed that all metals are not taken
326 up from the medium by *P. aeruginosa* cells with the same efficiency. Metals accumulated in the
327 cells depending on the surrounding environment. Among many elements, one of the most
328 efficiently extracted metals in succinate medium was Fe, with a concentration factor reaching
329 3,200. Certain toxic elements, such as nickel or chromium, can be incorporated into the mineral
330 structure of asbestos, depending on the metals present in the mines from which it is extracted.
331 Serpentine soils often contain large amounts of nickel, which can be found in the chemical
332 composition of chrysotile fibers through substitution with Mg (Chardot-Jacques et al., 2013).
333 These toxic elements can be dissolved together with Fe during bacterially-promoted dissolution
334 of minerals. Schalk et al. (2011) showed that siderophores produced by *P. aeruginosa* can
335 chelate other metals, although at a lower efficiency. Thus, these toxic metals can be solubilized
336 due to bacterial activity. In addition to their role in iron acquisition, siderophores can also
337 prevent the accumulation of toxic metals in *P. aeruginosa* cells, thus preserving the equilibrium

of the metallome in a polluted environment. Thus, siderophore-producing *Pseudomonas* could be used to remove toxic heavy metals from asbestos waste, avoiding environmental pollution.

In contrast to iron, there was no difference in the Mg content in solution in the absence or presence of bacteria, suggesting that the bacteria may not influence Mg dissolution from asbestos fibers, whereas the medium was likely responsible for solubilization of the magnesium. We thus determined the magnesium requirements for *P. aeruginosa.* The number of bacteria gradually increased when the medium was supplemented with Mg (**Figure 2**). Bacterial growth was restored in 0.05 mg.L-1 Mg under the tested condition, whereas optimal growth required 0.5 to 2 mg.L-1 Mg. The incubation of FAW in succinate medium without bacteria, as a control in the experiment of Figure 1, resulted in a dissolved Mg concentration of 1.5 mg.L-1 (data not shown). Given that the media was Mg-poor, the bacteria could only grow if Mg was obtained from the solid phase FAW and at a sufficient concentration to sustain their growth.

3.2 Long-term alteration of chrysotile gypsum by *Pseudomonas aeruginosa*

Our results show that bacteria can access Fe and Mg from FAW over a short period of time (24 h). This suggest that the materials were altered under these conditions. We thus tested whether repeated cycles could continuously provide these elements for bacterial growth. Short contact cycles of 8 h were performed to conform to the exponential growth phase and avoid biofilm formation. We observed a higher number of bacteria when the media was supplemented with FAW until the fourth renewal cycle (C1 to C4), whereas similar growth to that in media without FAW was observed for C5 and C6. The following two cycles (C7 and C8) showed a second stimulation of growth, which no longer occurred at later cycles until the end of the experiment (C16) (**Figure 3A**). Such enhancement of growth could correlate with various sites of extraction from the FAW. Siderophores often bind to minerals and their high affinity for iron

binding or adsorption is a prerequisite to dissolve iron. During the first cycles, iron and magnesium absorbed or present in the brucite layer could be easily dissolved, whereas elements present in the silica layer could be slow to be released. Our results tend to confirm this hypothesis, as already suggested by Mohanty et al. (2018) on the chrysotile ore. In the following cycles, there was not ready access to these nutrients present in the FAW, as there was no stimulation of growth for two cycles (C5/C6). More cycles or longer exposure appears to be required to restore the benefit provided by FAW to bacterial growth, probably due to the seeking of the essential elements in the deeper layers of the asbestos fiber. The absence of an effect after the ninth cycle may be attributed to the time of contact, which may have been too short.

Analysis of chrysotile fibers by STEM-EDX (Figure 3B, C, D, E) showed a decrease in iron content after long-term alteration with *P. aeruginosa* and confirms that iron was removed from the fiber structure. These results confirm the active dissolution of iron driven by *Pseudomonas.* Iron removal could reduce the toxicity of asbestos fibers as showed by Mohanty et al. (2018). The potential detoxification of asbestos waste by bacteria could be considered to reduce the health problems associated with exposure to toxic fibers at contaminated sites. However, a similar magnesium content was observed, with or without *P. aeruginosa.* This is likely associated with equivalent dissolution between the two conditions, corroborating the impact of the succinate medium in solubilizing magnesium.

3.3 Role and involvement of pyoverdine and pyochelin in altering FAW

P. aeruginosa is a bacterium that produces the two siderophores pyoverdine and pyochelin. We showed the ability of this bacterium to extract elements from FAW and next investigated the involvement of these two siderophores in this process. Given the ability of succinate medium to solubilize magnesium from FAW, further experiments were performed

using another minimal medium restricted in iron, CAA. When needed, the medium was not supplemented with magnesium (CAA-Mg). This medium showed weak magnesium dissolution (1 mg.L-1) relative to the succinate medium (11 mg.L-1) after 24 h of incubation with FAW (data not shown).

Among the biosynthetic enzymes for pyochelin and pyoverdine, we tagged PvdJ and PchA with the fluorescent protein mCherry to follow the synthesis of proteins involved in siderophore production in the presence of FAW (**Figure 4**). Allelic exchange was used to produce a strain expressing PvdJ with mCherry fused to its C-terminus (*PvdJmcherry*). Chromosomal insertion was chosen to maintain expression levels close to those of the wildtype strain. This strain grew as well as the parental PAO1 strain and showed the same level of pyoverdine production as that of the parental strain in iron-depleted CAA medium (Supplementary Figure 1).

After 24 h of incubation in CAA medium, we observed high fluorescence for both biosynthetic enzymes PvdJ (1,064) and PchA (1,331) due to iron depletion from the medium. However, the fluorescence of PvdJ-mCherry (143) and PchA-mCherry (309) was low in CAA-Mg medium, related to the absence of bacterial growth. Both biosynthetic enzymes were highly expressed (547 for PvdJ and 785 for PchA) in CAA medium supplemented with FAW, but the levels remained significantly lower than those of the positive control (CAA). This is consistent with the repression of siderophore production shown in **Figure 1A**, related to iron release from FAW. These results confirm expression of the siderophore pathways in the presence of asbestos.

We next investigated the role of each siderophore in iron and magnesium dissolution from FAW using *P. aeruginosa* strains producing both endogenous siderophores (WT), no pyoverdine (ΔPVD), no pyochelin (ΔPCH), or neither of the two siderophores (2Δ). FAW

407 samples were incubated in CAA-Mg with the WT or mutants and the iron and magnesium
408 content in the supernatants and bacterial cells measured. There was no difference between the
409 growth of the WT and mutant strains (Supplementary Figure 2). Weak iron dissolution (0.08
410 mg.L-1) occurred in the control CAA-Mg medium, whereas we observed significantly higher
411 iron concentrations during the growth of the WT (0.28 mg.L-1) or single mutants ΔPVD (0.26
412 mg.L-1) or ΔPCH (0.23 mg.L-1) (**Figure 5A**). The absence of a difference in iron extraction
413 between these strains shows that the absence of one of the two siderophores can be compensated
414 by the production of the other. Only 0.09 mg.L-1 iron was measured in the absence of both
415 pyoverdine and pyochelin, similar to the concentration in the control CAA-Mg. This result
416 shows that both siderophores are involved in iron removal from fibers and that the absence of the
417 siderophores greatly reduces iron dissolution. One of the common weathering processes for
418 fungi, plants, and bacteria in the interaction with minerals is siderophore production. For
419 example, siderophore production by *Pseudomonas mendocina* can solubilize iron from goethite,
420 hematite, and ferrihydrite (Hersman et al., 2001). Ferret et al. (2014) reported the ability of
421 *Pseudomonas aeruginosa* to extract iron from smectite, linked with siderophore production.
422 Bacterial metabolism can therefore mobilize elements from various minerals and the use of
423 siderophores as chelating compounds can be considered to be a major mechanism of such
424 alterations. Asbestos minerals, although highly resistant to weathering, have been reported to be
425 biodegraded by a few species of bacteria. Yao et al. (2013) showed, for example, that *Bacillus*
426 *mucilaginosus* was able to accelerate serpentine powder dissolution due to ligand production.
427 Recently, Gram-negative bacteria, including some identified by the authors as probably a
428 *Staphylococcus*, were isolated from asbestos rock and asbestos-contaminated soil samples. These
429 isolates showed their ability to reduce the iron content of asbestos fibers (Bhattacharya et al.,

2015). Further study of previously isolated Gram-positive bacteria showed that these bacteria synthesize siderophores, with no indication of the structure of the produced compounds (Bhattacharya et al., 2016). Siderophore production is a common mechanism already described in the bacterial and fungal weathering of asbestos (Daghino et al., 2010; Rajkumar et al., 2009). Several studies have focused on the effect of the siderophore deferoxamine, produced by *Streptomyces pilosus,* on raw asbestos fibers and showed this siderophore to efficiently remove iron (Chao and Aust, 1994; Mohanty et al., 2018). Our results confirm the involvement of siderophores in altering asbestos and show that the pyoverdine and pyochelin pathways play an important role in iron removal from FAW. The use of siderophore pathways in a bacterial bioremediation process could allow the development of eco-friendly asbestos treatment, avoiding the continuing disposal of such waste in landfills. In addition to iron, we investigated the role of these two siderophores in magnesium dissolution from FAW (**Figure 5B**). The concentration of dissolved magnesium measured in experiments with the WT and mutants of *P. aeruginosa* was not significantly different. A well-known parameter described to influence the dissolution of the chrysotile brucite layer is pH (Choi and Smith, 1972; Gronow, 1987). Here, the pH changed from 7.50 to 8.40. Thus, it is likely that it did not influence the process, whereas it is probably linked to the involvement of other mechanisms, such as organic-acid production. Indeed, during growth, bacteria may secrete various metabolites, such as oxalic, succinic, formic, or lactic acid, depending on the carbon substrate present in the medium. The dissolution of chrysotile by organic acids is well known and has already been described in several studies. Oxalic acid, for example, can dissolve the brucite layer in chrysotile fibers (Rozalen et al., 2014; Thomassin et al., 1977). In our study, the alteration of asbestos may be the effect of a ligand-controlled dissolution mechanism driven by the siderophores and other organic ligands, depending on a

surface-controlled process that is a function of the surface concentration of the adsorbed ligands (Furrer and Stumm, 1986; Mohanty et al., 2018) and the solution saturation state.

4. Conclusion

Here, we report, for the first time, the acquisition of iron and magnesium from flocking asbestos waste by *Pseudomonas aeruginosa* and the involvement of siderophores. The presence of chrysotile-gypsum promoted the growth of *P. aeruginosa* in correlation with greater iron dissolution in the presence of the bacteria. Active dissolution of iron content from asbestos fibers was driven by *Pseudomonas* in a long-term alteration experiment of chrysotile-gypsum. Moreover, we clearly demonstrate the role and involvement of the siderophores, pyoverdine and pyochelin, in altering flocking asbestos. Indeed, the siderophore biosynthetic pathways were expressed in the presence of chrysotile-gypsum and the absence of both siderophores significantly reduced iron removal from asbestos waste. Our results show that FAW can serve as nutrient sources for bacteria using siderophores for iron release. The biodegradation of asbestos by siderophore-producing *Pseudomonas* could be an eco-friendly bioremediation process that could be used to treat loose asbestos waste and reduce asbestos-related environmental and health problems.

Acknowledgements

This work was supported by the French Environment and Energy Management Agency (ADEME) and the SOMEZ (Société Méditerranéenne des Zéolithes).

References

474 Aguado-Santacruz, G.A., Moreno-Gómez, B., Jiménez-Francisco, B., García-Moya, E.,
475 Preciado-Ortiz, R.E., 2012. Impact of the microbial siderophores and phytosiderophores
476 on the iron assimilation by plants: a synthesis. Revista Fitotecnia Mexicana 35, 9–21.
477 Albrecht-Gary, A.-M., Blanc, S., Rochel, N., Ocaktan, A.Z., Abdallah, M.A., 1994. Bacterial
478 Iron Transport: Coordination Properties of Pyoverdin PaA, a Peptidic Siderophore of
479 Pseudomonas aeruginosa. Inorg. Chem. 33, 6391–6402.
480 https://doi.org/10.1021/ic00104a059
481 Andrews, S.C., Robinson, A.K., Rodríguez-Quiñones, F., 2003. Bacterial iron homeostasis.
482 FEMS Microbiol Rev 27, 215–237. https://doi.org/10.1016/S0168-6445(03)00055-X
483 Beveridge, T.J., Makin, S.A., Kadurugamuwa, J.L., Li, Z., 1997. Interactions between biofilms
484 and the environment. FEMS Microbiol Rev 20, 291–303. https://doi.org/10.1111/j.1574-
485 6976.1997.tb00315.x
486 Bhattacharya, S., John, P.J., Ledwani, L., 2016. Fungal weathering of asbestos in semi arid
487 regions of India. Ecotoxicology and Environmental Safety 124, 186–192.
488 https://doi.org/10.1016/j.ecoenv.2015.10.022
489 Bhattacharya, S., John, P.J., Ledwani, L., 2015. Bacterial Weathering of Asbestos. Silicon 7,
490 419–431. https://doi.org/10.1007/s12633-014-9260-9
491 Brandel, J., Humbert, N., Elhabiri, M., Schalk, I.J., Mislin, G.L.A., Albrecht-Gary, A.-M., 2012.
492 Pyochelin, a siderophore of Pseudomonas aeruginosa: Physicochemical characterization
493 of the iron(III), copper(II) and zinc(II) complexes. Dalton Trans. 41, 2820–2834.
494 https://doi.org/10.1039/C1DT11804H
495 Braud, A., Hoegy, F., Jezequel, K., Lebeau, T., Schalk, I.J., 2009. New insights into the metal
496 specificity of the Pseudomonas aeruginosa pyoverdine–iron uptake pathway.

497 Environmental Microbiology 11, 1079–1091. https://doi.org/10.1111/j.1462-
498 2920.2008.01838.x
499 Budzikiewicz, H., 2004. Siderophores of the Pseudomonadaceae sensu stricto (Fluorescent and
500 Non-Fluorescent Pseudomonas spp.), in: Budzikiewicz, H., Flessner, T., Jautelat, R.,
501 Scholz, U., Winterfeldt, E., Herz, W., Falk, H., Kirby, G.W. (Eds.), Progress in the
502 Chemistry of Organic Natural Products, Progress in the Chemistry of Organic Natural
503 Products. Springer Vienna, Vienna, pp. 81–237. https://doi.org/10.1007/978-3-7091-
504 0581-8_2
505 Budzikiewicz, H., 1997. Siderophores of Fluorescent Pseudomonads. Z. Naturforschung C 52,
506 713–720. https://doi.org/10.1515/znc-1997-11-1201
507 Budzikiewicz, H., Schäfer, M., Fernández, D.U., Matthijs, S., Cornelis, P., 2007.
508 Characterization of the chromophores of pyoverdins and related siderophores by
509 electrospray tandem mass spectrometry. Biometals 20, 135–144.
510 https://doi.org/10.1007/s10534-006-9021-3
511 Chao, C.C., Aust, A.E., 1994. Effect of Long-Term Removal of Iron from Asbestos by
512 Desferrioxamine B on Subsequent Mobilization by Other Chelators and Induction of
513 DNA Single-Strand Breaks. Archives of Biochemistry and Biophysics 308, 64–69.
514 https://doi.org/10.1006/abbi.1994.1009
515 Chardot-Jacques, V., Calvaruso, C., Simon, B., Turpault, M.-P., Echevarria, G., Morel, J.-L.,
516 2013. Chrysotile Dissolution in the Rhizosphere of the Nickel Hyperaccumulator
517 Leptoplax emarginata. Environmental Science & Technology 47, 2612–2620.
518 https://doi.org/10.1021/es301229m

519 Choi, I., Smith, R.W., 1972. Kinetic study of dissolution of asbestos fibers in water. Journal of
520 Colloid and Interface Science 40, 253–262. https://doi.org/10.1016/0021-9797(72)90014-
521 8
522 Cocozza, C., Ercolani, G.L., 1997. Siderophore production and associated characteristics in
523 rhizosphere and non-rhizosphere fluorescent pseudomonads. Annali di microbiol.
524 enzimol. 47, 17–28.
525 Cornelis, P., Dingemans, J., 2013. Pseudomonas aeruginosa adapts its iron uptake strategies in
526 function of the type of infections. Front. Cell. Infect. Microbiol. 3, 75.
527 https://doi.org/10.3389/fcimb.2013.00075
528 Cornell, R.M., Schwertmann, U., 2003. The Iron Oxides: Structure, Properties, Reactions,
529 Occurrences and Uses. John Wiley & Sons.
530 Cunrath, O., Gasser, V., Hoegy, F., Reimmann, C., Guillon, L., Schalk, I.J., 2015. A cell
531 biological view of the siderophore pyochelin iron uptake pathway in Pseudomonas
532 aeruginosa. Environmental Microbiology 17, 171–185. https://doi.org/10.1111/1462-
533 2920.12544
534 Cunrath, O., Geoffroy, V.A., Schalk, I.J., 2016. Metallome of Pseudomonas aeruginosa: a role
535 for siderophores. Environmental Microbiology 18, 3258–3267.
536 https://doi.org/10.1111/1462-2920.12971
537 Daghino, S., Martino, E., Perotto, S., 2010. Fungal weathering and implications in the
538 solubilization of metals from soil and from asbestos fiber. Current research, technology
539 and education topics in applied microbiology and microbial biotechnology 1, 329–338.
540 Demange, P., Wendenbaum, S., Linget, C., Mertz, C., Cung, M.T., Dell, A., Abdallah, M.A.,
541 1990. Bacterial siderophores : structure and NMR assignment of pyoverdins Pa,

542 siderophores ofPseudomonas aeruginosa ATCC 15692. Biol Metals 3, 155–170.
543 https://doi.org/10.1007/BF01140574
544 Duckworth, O.W., Bargar, J.R., Sposito, G., 2009. Coupled biogeochemical cycling of iron and
545 manganese as mediated by microbial siderophores. Biometals 22, 605–613.
546 https://doi.org/10.1007/s10534-009-9220-9
547 Dumas, Z., Ross-Gillespie, A., Kümmerli, R., 2013. Switching between apparently redundant
548 iron-uptake mechanisms benefits bacteria in changeable environments. Proc. Biol. Sci.
549 280, 20131055. https://doi.org/10.1098/rspb.2013.1055
550 Ferret, C., Sterckeman, T., Cornu, J.-Y., Gangloff, S., Schalk, I.J., Geoffroy, V.A., 2014.
551 Siderophore-promoted dissolution of smectite by fluorescent Pseudomonas.
552 Environmental Microbiology Reports 6, 459–467. https://doi.org/10.1111/1758-
553 2229.12146
554 Folschweiller, N., Gallay, J., Vincent, M., Abdallah, M.A., Pattus, F., Schalk, I.J., 2002. The
555 Interaction between Pyoverdin and Its Outer Membrane Receptor in Pseudomonas
556 aeruginosa Leads to Different Conformers: A Time-Resolved Fluorescence Study.
557 Biochemistry 41, 14591–14601. https://doi.org/10.1021/bi0259711
558 Fuchs, R., Budzikiewicz, H., 2001. Structural Studies of Pyoverdins by Mass Spectrometry.
559 Curr. Org. Chem. 5, 265–288. https://doi.org/10.2174/1385272013375562
560 Furrer, G., Stumm, W., 1986. The coordination chemistry of weathering: I. Dissolution kinetics
561 of δ-Al2O3 and BeO. Geochimica et Cosmochimica Acta 50, 1847–1860.
562 https://doi.org/10.1016/0016-7037(86)90243-7
563 Gasser, V., Baco, E., Cunrath, O., August, P.S., Perraud, Q., Zill, N., Schleberger, C., Schmidt,
564 A., Paulen, A., Bumann, D., Mislin, G.L.A., Schalk, I.J., 2016. Catechol siderophores

565 repress the pyochelin pathway and activate the enterobactin pathway in Pseudomonas
566 aeruginosa: an opportunity for siderophore–antibiotic conjugates development.
567 Environmental Microbiology 18, 819–832. https://doi.org/10.1111/1462-2920.13199
568 Gasser, V., Guillon, L., Cunrath, O., Schalk, Isabelle.J., 2015. Cellular organization of
569 siderophore biosynthesis in Pseudomonas aeruginosa: Evidence for siderosomes. Journal
570 of Inorganic Biochemistry, 12th European Biological Inorganic Chemistry Conference
571 (EuroBIC 12) in Zurich, Switzerland, August 24-28, 2014 148, 27–34.
572 https://doi.org/10.1016/j.jinorgbio.2015.01.017
573 Gold J, Amandusson H, Krozer A, Kasemo B, Ericsson T, Zanetti G, Fubini B, 1997. Chemical
574 characterization and reactivity of iron chelator-treated amphibole asbestos.
575 Environmental Health Perspectives 105, 1021–1030.
576 https://doi.org/10.1289/ehp.97105s51021
577 Goldberg, J.B., 2000. Pseudomonas: global bacteria. Trends Microbiol. 8, 55–57.
578 Groisman, E.A., Hollands, K., Kriner, M.A., Lee, E.-J., Park, S.-Y., Pontes, M.H., 2013.
579 Bacterial Mg2+ Homeostasis, Transport, and Virulence. Annual Review of Genetics 47,
580 625–646. https://doi.org/10.1146/annurev-genet-051313-051025
581 Gronow, J.R., 1987. The dissolution of asbestos fibres in water. Clay Minerals 22, 21–35.
582 https://doi.org/10.1180/claymin.1987.022.1.03
583 Hardy, J.A., Aust, A.E., 1995. The effect of iron binding on the ability of crocidolite asbestos to
584 catalyze DNA single-strand breaks. Carcinogenesis 16, 319–325.
585 https://doi.org/10.1093/carcin/16.2.319

586 Heldal, M., Norland, S., Tumyr, O., 1985. X-ray microanalytic method for measurement of dry
587 matter and elemental content of individual bacteria. Appl. Environ. Microbiol. 50, 1251–
588 1257.
589 Herrero, M., Lorenzo, V. de, Timmis, K.N., 1990. Transposon vectors containing non-antibiotic
590 resistance selection markers for cloning and stable chromosomal insertion of foreign
591 genes in gram-negative bacteria. Journal of Bacteriology 172, 6557–6567.
592 https://doi.org/10.1128/jb.172.11.6557-6567.1990
593 Hersman, L., Lloyd, T., Sposito, G., 1995. Siderophore-promoted dissolution of hematite.
594 Geochimica et Cosmochimica Acta 59, 3327–3330. https://doi.org/10.1016/0016-
595 7037(95)00221-K
596 Hersman, L.E., Forsythe, J.H., Ticknor, L.O., Maurice, P.A., 2001. Growth of Pseudomonas
597 mendocina on Fe(III) (Hydr)Oxides. Appl. Environ. Microbiol. 67, 4448–4453.
598 https://doi.org/10.1128/AEM.67.10.4448-4453.2001
599 Hoegy, F., Lee, X., Noel, S., Rognan, D., Mislin, G.L.A., Reimmann, C., Schalk, I.J., 2009.
600 Stereospecificity of the Siderophore Pyochelin Outer Membrane Transporters in
601 Fluorescent Pseudomonads. J. Biol. Chem. 284, 14949–14957.
602 https://doi.org/10.1074/jbc.M900606200
603 Kalinowski, B.E., Liermann, L.J., Givens, S., Brantley, S.L., 2000. Rates of bacteria-promoted
604 solubilization of Fe from minerals: a review of problems and approaches. Chemical
605 Geology 169, 357–370. https://doi.org/10.1016/S0009-2541(00)00214-X
606 Kraemer, S.M., 2004. Iron oxide dissolution and solubility in the presence of siderophores.
607 Aquat. Sci. 66, 3–18. https://doi.org/10.1007/s00027-003-0690-5

608 Liermann, L.J., Barnes, A.S., Kalinowski, B.E., Zhou, X., Brantley, S.L., 2000.
609 Microenvironments of pH in biofilms grown on dissolving silicate surfaces. Chemical
610 Geology 171, 1–16. https://doi.org/10.1016/S0009-2541(00)00202-3
611 Maurice, P.A., Haack, E.A., Mishra, B., 2009. Siderophore sorption to clays. Biometals 22, 649–
612 658. https://doi.org/10.1007/s10534-009-9242-3
613 Mohanty, S.K., Gonneau, C., Salamatipour, A., Pietrofesa, R.A., Casper, B., Christofidou-
614 Solomidou, M., Willenbring, J.K., 2018. Siderophore-mediated iron removal from
615 chrysotile: Implications for asbestos toxicity reduction and bioremediation. Journal of
616 Hazardous Materials 341, 290–296. https://doi.org/10.1016/j.jhazmat.2017.07.033
617 Neilands, J.B., 1981. Microbial Iron Compounds. Annual Review of Biochemistry 50, 715–731.
618 https://doi.org/10.1146/annurev.bi.50.070181.003435
619 Ojeda, L., Keller, G., Muhlenhoff, U., Rutherford, J.C., Lill, R., Winge, D.R., 2006. Role of
620 Glutaredoxin-3 and Glutaredoxin-4 in the Iron Regulation of the Aft1 Transcriptional
621 Activator in Saccharomyces cerevisiae. J. Biol. Chem. 281, 17661–17669.
622 https://doi.org/10.1074/jbc.M602165200
623 Poser, I., Rahman, Q., Lohani, M., Yadav, S., Becker, H.-H., Weiss, D.G., Schiffmann, D.,
624 Dopp, E., 2004. Modulation of genotoxic effects in asbestos-exposed primary human
625 mesothelial cells by radical scavengers, metal chelators and a glutathione precursor.
626 Mutation Research/Genetic Toxicology and Environmental Mutagenesis 559, 19–27.
627 https://doi.org/10.1016/j.mrgentox.2003.12.006
628 Rajkumar, M., Vara Prasad, M.N., Freitas, H., Ae, N., 2009. Biotechnological applications of
629 serpentine soil bacteria for phytoremediation of trace metals. Crit. rev. biotechnol. 29,
630 120–130. https://doi.org/10.1080/07388550902913772

631 Rietsch, A., Vallet-Gely, I., Dove, S.L., Mekalanos, J.J., 2005. ExsE, a secreted regulator of type
632 III secretion genes in Pseudomonas aeruginosa. PNAS 102, 8006–8011.
633 https://doi.org/10.1073/pnas.0503005102
634 Rosenberg, D.R., Maurice, P.A., 2003. Siderophore adsorption to and dissolution of kaolinite at
635 pH 3 to 7 and 22°C. Geochimica et Cosmochimica Acta 67, 223–229.
636 https://doi.org/10.1016/S0016-7037(02)01082-7
637 Rozalen, M., Ramos, M.E., Fiore, S., Gervilla, F., Huertas, F.J., 2014. Effect of oxalate and pH
638 on chrysotile dissolution at 25 °C: An experimental study. American Mineralogist 99,
639 589–600. https://doi.org/10.2138/am.2014.4636
640 Schalk, I.J., Hannauer, M., Braud, A., 2011. New roles for bacterial siderophores in metal
641 transport and tolerance. Environmental Microbiology 13, 2844–2854.
642 https://doi.org/10.1111/j.1462-2920.2011.02556.x
643 Schvartz, C., Decroux, J., Muller, J.-C., 2005. Guide de la fertilisation raisonnée: grandes
644 cultures et prairies. France Agricole Editions.
645 Stover, C.K., Pham, X.Q., Erwin, A.L., Mizoguchi, S.D., Warrener, P., Hickey, M.J., Brinkman,
646 F.S.L., Hufnagle, W.O., Kowalik, D.J., Lagrou, M., Garber, R.L., Goltry, L., Tolentino,
647 E., Westbrock-Wadman, S., Yuan, Y., Brody, L.L., Coulter, S.N., Folger, K.R., Kas, A.,
648 Larbig, K., Lim, R., Smith, K., Spencer, D., Wong, G.K.-S., Wu, Z., Paulsen, I.T.,
649 Reizer, J., Saier, M.H., Hancock, R.E.W., Lory, S., Olson, M.V., 2000. Complete genome
650 sequence of Pseudomonas aeruginosa PAO1, an opportunistic pathogen. Nature 406,
651 959–964. https://doi.org/10.1038/35023079

652 Thomassin, J.H., Goni, J., Baillif, P., Touray, J.C., Jaurand, M.C., 1977. An XPS study of the
653 dissolution kinetics of chrysotile in 0.1 N oxalic acid at different temperatures. Phys
654 Chem Minerals 1, 385–398. https://doi.org/10.1007/BF00308848
655 Toyokuni, S., 2009. Mechanisms of asbestos-induced carcinogenesis. Nagoya journal of medical
656 science 71, 1–10.
657 Tseng, C.-F., Burger, A., Mislin, G.L.A., Schalk, I.J., Yu, S.S.-F., Chan, S.I., Abdallah, M.A.,
658 2006. Bacterial siderophores: the solution stoichiometry and coordination of the Fe(III)
659 complexes of pyochelin and related compounds. J Biol Inorg Chem 11, 419–432.
660 https://doi.org/10.1007/s00775-006-0088-7
661 Virta, R.L., 2002. Asbestos: geology, mineralogy, mining, and uses. US Department of the
662 Interior. US Geological Survey.
663 Wang, D., Cullimore, D.R., 2010. Bacteriological challenges to asbestos cement water
664 distribution pipelines. Journal of Environmental Sciences 22, 1203–1208.
665 https://doi.org/10.1016/S1001-0742(09)60239-4
666 Wang, D., Cullimore, R., Hu, Y., Chowdhury, R., 2011. Biodeterioration of asbestos cement
667 (AC) pipe in drinking water distribution systems. International Biodeterioration &
668 Biodegradation 65, 810–817. https://doi.org/10.1016/j.ibiod.2011.05.004
669 Yao, M., Lian, B., Teng, H.H., Tian, Y., Yang, X., 2013. Serpentine Dissolution in the Presence
670 of Bacteria Bacillus mucilaginosus. Geomicrobiology Journal 30, 72–80.
671 https://doi.org/10.1080/01490451.2011.653087
672

673 **Figure legends**

674 **Figure 1.** Growth of *Pseudomonas aeruginosa* PAO1 during 24 h in succinate medium with
675 (Succ) or without magnesium (Succ-Mg), in the presence or absence of chrysotile-gypsum
676 (CHR-GY) (A). Quantification of pyoverdine in supernatants after 24 h of *P. aeruginosa* PAO1
677 growth in Succ or Succ-Mg, with or without CHR-GY (B). Evolution of iron concentration
678 extracted from chrysotile-gypsum waste over 24 h in the presence of *P. aeruginosa* PAO1 or
679 Succ-Mg (C). Total concentration of iron dissolved from chrysotile-gypsum after 24 h in the
680 presence of *P. aeruginosa* PAO1 or Succ-Mg. Iron was measured in the bacterial cells (Pellet)
681 and supernatants (D). Error bars indicate the standard deviations of the means of three or five
682 replicates. Bars with the same letter are not significantly different ($p > 0.05$, Kruskal-Wallis test
683 and Wilcoxon signed rank test, three or five replicates).

684 **Figure 2.** Growth of *Pseudomonas aeruginosa* PAO1 during 37.5 h in succinate medium
685 containing various concentrations of magnesium (0 to 2 $mg.L^{-1}$). Error bars indicate the standard
686 deviations of the means of three replicates.

687 **Figure 3.** Enumeration of *Pseudomonas aeruginosa* PAO1 during 16 growth cycles of 8 h in
688 succinate medium without magnesium (Succ-Mg), in the presence or absence of chrysotile-
689 gypsum (CHR-GY) (A). STEM images of chrysotile fibers before (B) and after (C) bacterial
690 contact. Atomic ratios of Mg/Si and Fe/Si before (control) and after contact of chrysotile-gypsum
691 with *P. aeruginosa* PAO1 (D). Mass percentage of iron, magnesium, and silicon before and after
692 contact of chrysotile-gypsum with *P. aeruginosa* PAO1 (E). Error bars indicate the standard
693 deviations of the means of three replicates.

694 **Figure 4.** Fluorescence of PvdJ-mCherry and PchA-mCherry after 24 h of *P. aeruginosa* PAO1
695 growth in casamino acids medium with (CAA) or without magnesium (CAA-Mg), in the

696 presence or absence of chrysotile-gypsum (CHR-GY). Error bars indicate the standard deviations
697 of the means of three or five replicates. Bars with the same letter are not significantly different (p
698 > 0.05, One-way ANOVA, three or five replicates).

699 **Figure 5.** Concentration of iron (A) and magnesium (B) dissolved from chrysotile-gypsum after
700 18 h in the presence of casamino acids medium without magnesium (CAA-Mg) as a control or
701 inoculated with the wildtype *Pseudomonas aeruginosa* PAO1 strain (WT), pyoverdine-deficient
702 strain (ΔPVD), pyochelin-deficient strain (ΔPCH), or pyoverdine- and pyochelin-deficient strain
703 (2Δ). Elements were measured in the bacterial cells (Pellet) and supernatants. Error bars indicate
704 the standard deviations of the means of three replicates. Bars with the same letter are not
705 significantly different ($p > 0.05$, One-way ANOVA and Kruskal-Wallis test, three replicates).
706

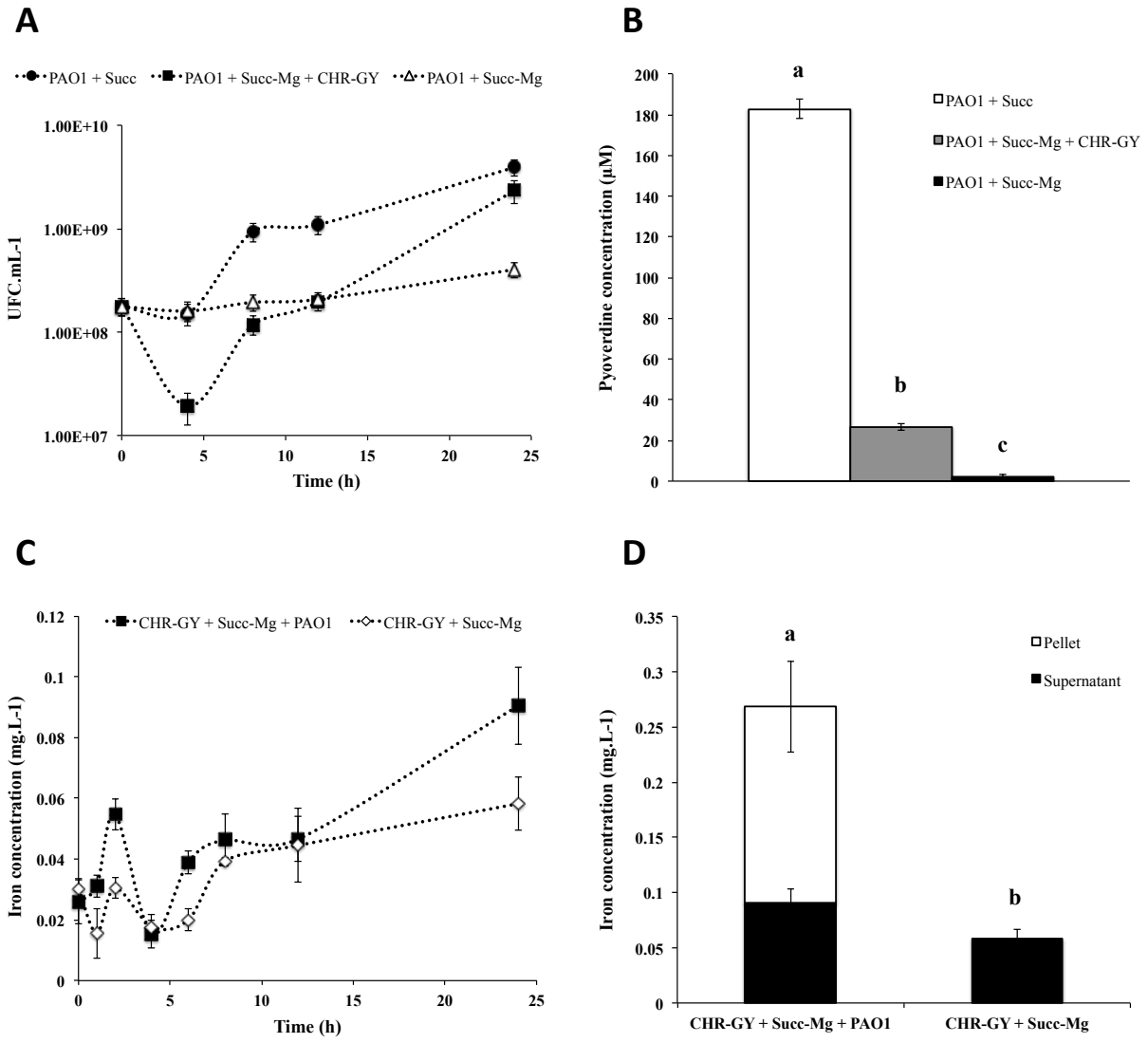

Figure 1: Growth of *Pseudomonas aeruginosa* PAO1 during 24 h in succinate medium with (Succ) or without magnesium (Succ-Mg), in the presence or absence of chrysotile-gypsum (CHR-GY) (A). Quantification of pyoverdine in supernatants after 24 h of *P. aeruginosa* PAO1 growth in Succ or Succ-Mg, with or without CHR-GY (B). Evolution of iron concentration extracted from chrysotile-gypsum waste over 24 h in the presence of *P. aeruginosa* PAO1 or Succ-Mg (C). Total concentration of iron dissolved from chrysotile-gypsum after 24 h in the presence of *P. aeruginosa* PAO1 or Succ-Mg. Iron was measured in the bacterial cells (Pellet) and supernatants (D). Error bars indicate the standard deviations of the means of three or five replicates. Bars with the same letter are not significantly different ($p > 0.05$, Kruskal-Wallis test and Wilcoxon signed rank test, three or five replicates).

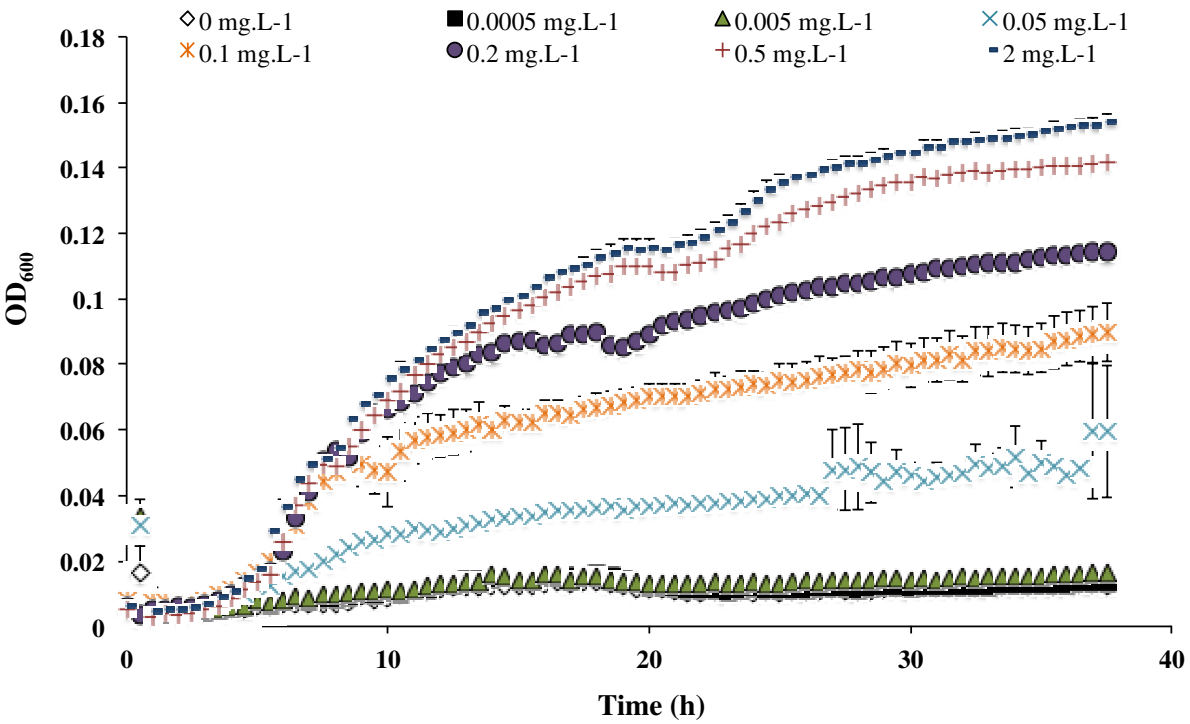

Figure 2: Growth of *Pseudomonas aeruginosa* PAO1 during 37.5 h in succinate medium containing various concentrations of magnesium (0 to 2 $mg.L^{-1}$). Error bars indicate the standard deviations of the means of three replicates.

In color print

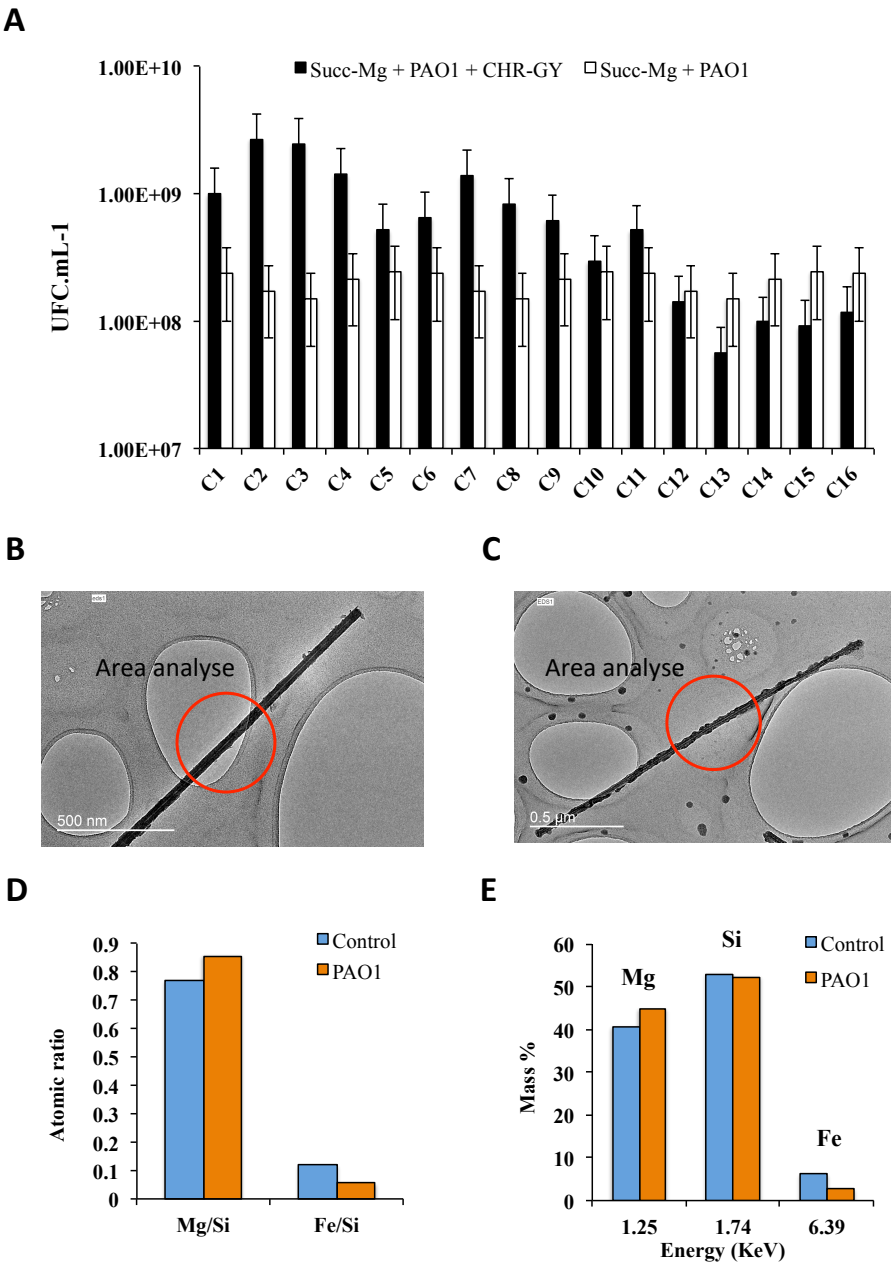

Figure 3: Enumeration of *Pseudomonas aeruginosa* PAO1 during 16 growth cycles of 8 h in succinate medium without magnesium (Succ-Mg), in the presence or absence of chrysotile-gypsum (CHR-GY) (A). STEM images of chrysotile fibers before (B) and after (C) bacterial contact. Atomic ratios of Mg/Si and Fe/Si before (control) and after contact of chrysotile-gypsum with *P. aeruginosa* PAO1 (D). Mass percentage of iron, magnesium, and silicon before and after contact of chrysotile-gypsum with *P. aeruginosa* PAO1 (E). Error bars indicate the standard deviations of the means of three replicates.

In color print

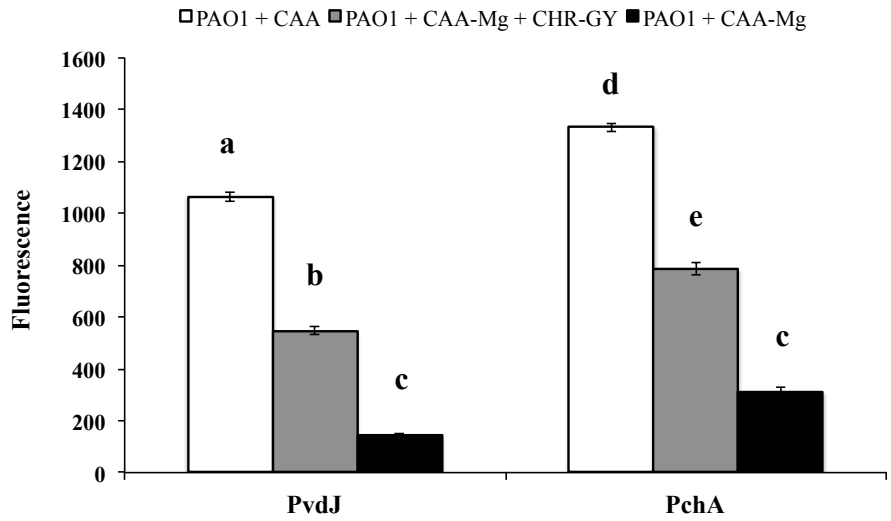

Figure 4: Fluorescence of PvdJ-mCherry and PchA-mCherry after 24 h of *P. aeruginosa* PAO1 growth in casamino acids medium with (CAA) or without magnesium (CAA-Mg), in the presence or absence of chrysotile-gypsum (CHR-GY). Error bars indicate the standard deviations of the means of three or five replicates. Bars with the same letter are not significantly different ($p > 0.05$, One-way ANOVA, three or five replicates).

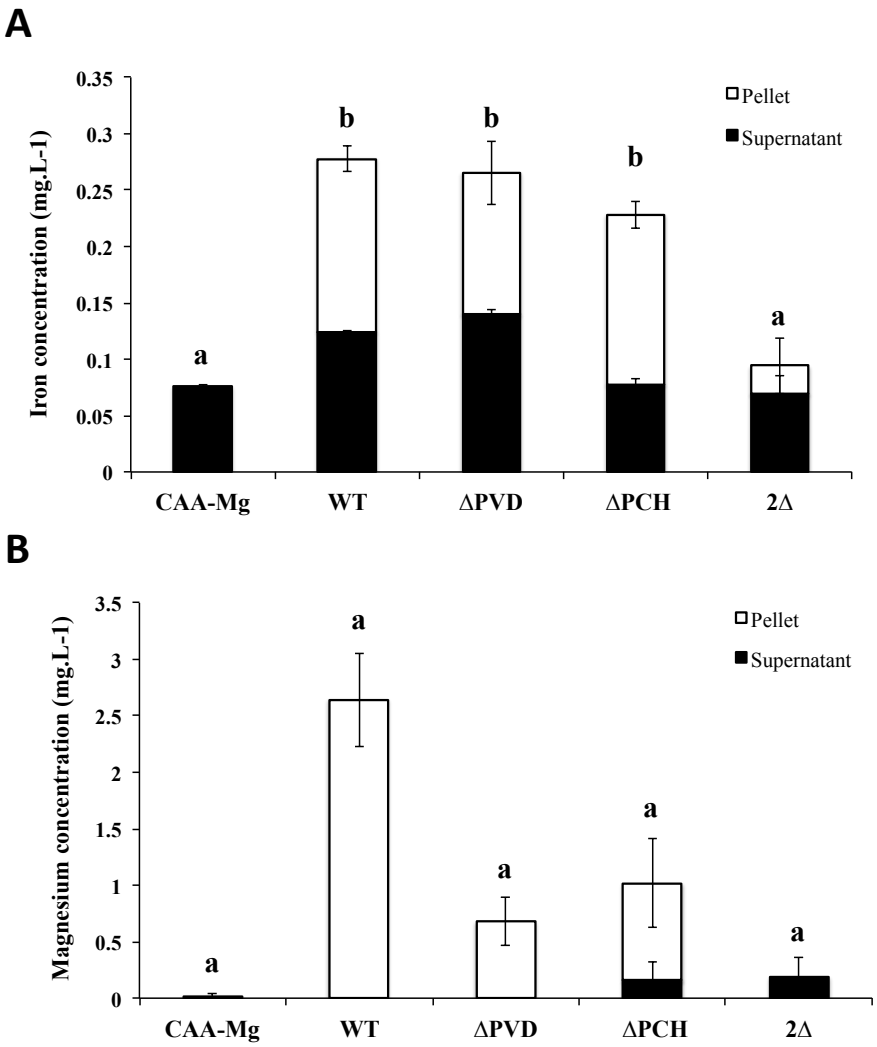

Figure 5: Concentration of iron (A) and magnesium (B) dissolved from chrysotile-gypsum after 18 h in the presence of casamino acids medium without magnesium (CAA-Mg) as a control or inoculated with the wildtype *Pseudomonas aeruginosa* PAO1 strain (WT), pyoverdine-deficient strain (ΔPVD), pyochelin-deficient strain (ΔPCH), or pyoverdine- and pyochelin-deficient strain (2Δ). Elements were measured in the bacterial cells (Pellet) and supernatants. Error bars indicate the standard deviations of the means of three replicates. Bars with the same letter are not significantly different ($p > 0.05$, One-way ANOVA and Kruskal-Wallis test, three replicates).

Table 1: Strains and plasmids used in this study.

Strains and plasmids	Relevant characteristics	References
Pseudomonas aeruginosa		
PAO1	Wild-type strain	(Stover *et al.*, 2000)
Δ*pvdF*	PAO1; Δ*pvdF*	(Hoegy *et al.*, 2009)
Δ*pchA*	PAO1; Δ*pchA*	(Cunrath *et al.*, 2015)
Δ*pvdF*Δ*pchA*	PAO1; Δ*pvdF*Δ*pchA*	(Gasser *et al.*, 2016)
pvdJmcherry	Derivate of PAO1; *pvdjmcherry* chromosomally integrated	This study
pchAmcherry	PAO1; *pchAmcherry*	(Cunrath *et al.*, 2015)
Escherichia coli		
SM10	thi thr leu tonA lacY supE recA::RP4-2-Tc::Mu Km λpir	(Herrero *et al.*, 1990)
Plasmids		
pLG45	pME3088 pvdJmcherry with 700bp flanking region relative to mcherry	(Gasser *et al.*, 2015)
pEXG2	allelic exchange vector with pBR origin, gentamicin resistance, sacB	(Rietsch *et al*., 2005)
pEXG2 *pvdJmcherry*	pEXG2 carrying the sequence to insert mcherry tag in C-terminus of *pvdJ*	This study

Graphical Abstract

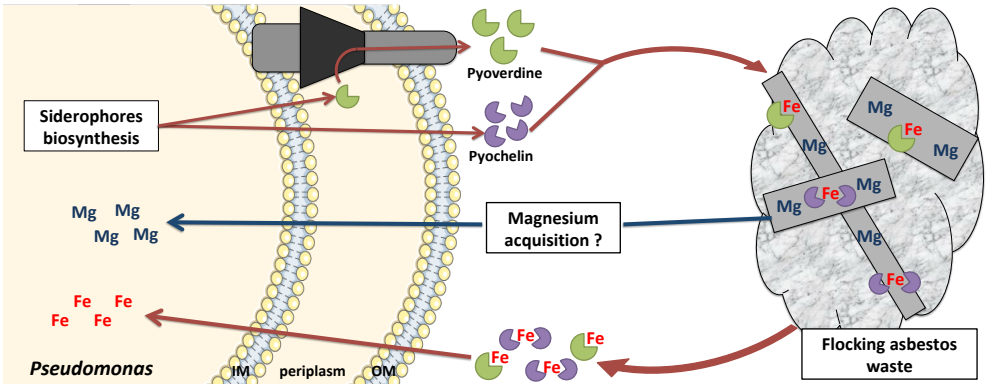

In color print